THE JOURNAL OF PHYSICAL CHEMISTRY A

 VOLUME 108, NUMBER 19, MAY 13, 2004

LETTERS

Optimal Control of Ionization Processes in NaK: Comparison between Theory and Experiment

Boris Schäfer-Bung, Roland Mitrić, and Vlasta Bonačić-Koutecký*

Institut für Chemie, Humboldt-Universität zu Berlin, Brook-Taylor-Strasse 2, D-12489 Berlin, Germany

Andreas Bartelt,† Cosmin Lupulescu, Albrecht Lindinger, Štefan Vajda,‡ Stefan M. Weber, and Ludger Wöste

Institut für Experimentalphysik, Freie Universität Berlin, Arnimallee 14, D-14195 Berlin, Germany

Received: February 25, 2004; In Final Form: March 12, 2004

We report a good agreement between the shapes of tailored pulses obtained theoretically and experimentally by using the optimal-control theory and the closed-loop learning technique to maximize the ionization yield in NaK. The theoretical pulse shapes are found to be robust regarding the choice of the initial guess. We assign the leading features of the pulse shapes to processes underlying the optimal control and reveal the mechanism which involves an electronic transition followed by a direct two-photon process and sequential one-photon processes at later times. We show that the optimal control not only serves for maximizing the desired yield but also as a tool for the analysis and the identification of the responsible processes.

I. Introduction

Tailored laser pulses are appropriate for exciting different superpositions of eigenstates by coherent control creating wave packets which are directed to a desired target state. Initiated originally by proposed different control schemes in the frequency[1] as well as in the time domain,[2−5] the development was followed by introducing a closed-loop learning control[5] (CLL). Advances achieved in pulse-shaping techniques opened new roads in the field, in particular concerning the control of chemical reactivity in complex systems.[6−9] However, the investigation of simple systems offers a possibility to learn how to use the control as a tool for analyzing the underlying processes. Therefore, metallic dimers[10−18] and diatomic molecules[19,20] have been studied in numerous contributions, since they are suitable model systems for verifying the scopes of different control schemes and they are accessible to experimental pulse shaping techniques.[21−32] Theoretical and experimental work using two-parameter control has been performed: In addition to the pump−probe time delay, the second control parameter involved the pump[10,21−22] and/or probe[11,14] wavelength, the pump−dump delay,[12,23−24] the laser power,[13] the chirp,[15,25] or temporal width[19] of the laser pulse. Optimal pump−dump control of K_2 has been carried out theoretically in order to maximize the population of certain vibrational levels of the ground electronic state using one electronic excited state as an intermediate pathway.[16−18] Concerning optimal control for the maximization of the ionization yield in alkali dimers, the experimental work using evolutionary algorithms[26−32] has prompted the theoretical investigations presented here.

* To whom correspondence may be addressed. Phone: +49-30-20935579. Fax: +49-30-20935573. E-mail: vbk@chemie.hu-berlin.de.

† Present address: Department of Chemistry, Princeton University, Princeton, NJ 08542.

‡ Present address: Argonne National Laboratory, Chemistry Division, 9700 South Cass Avenue, Argonne, IL 60439.

10.1021/jp049153p CCC: $27.50
Published on Web 04/17/2004

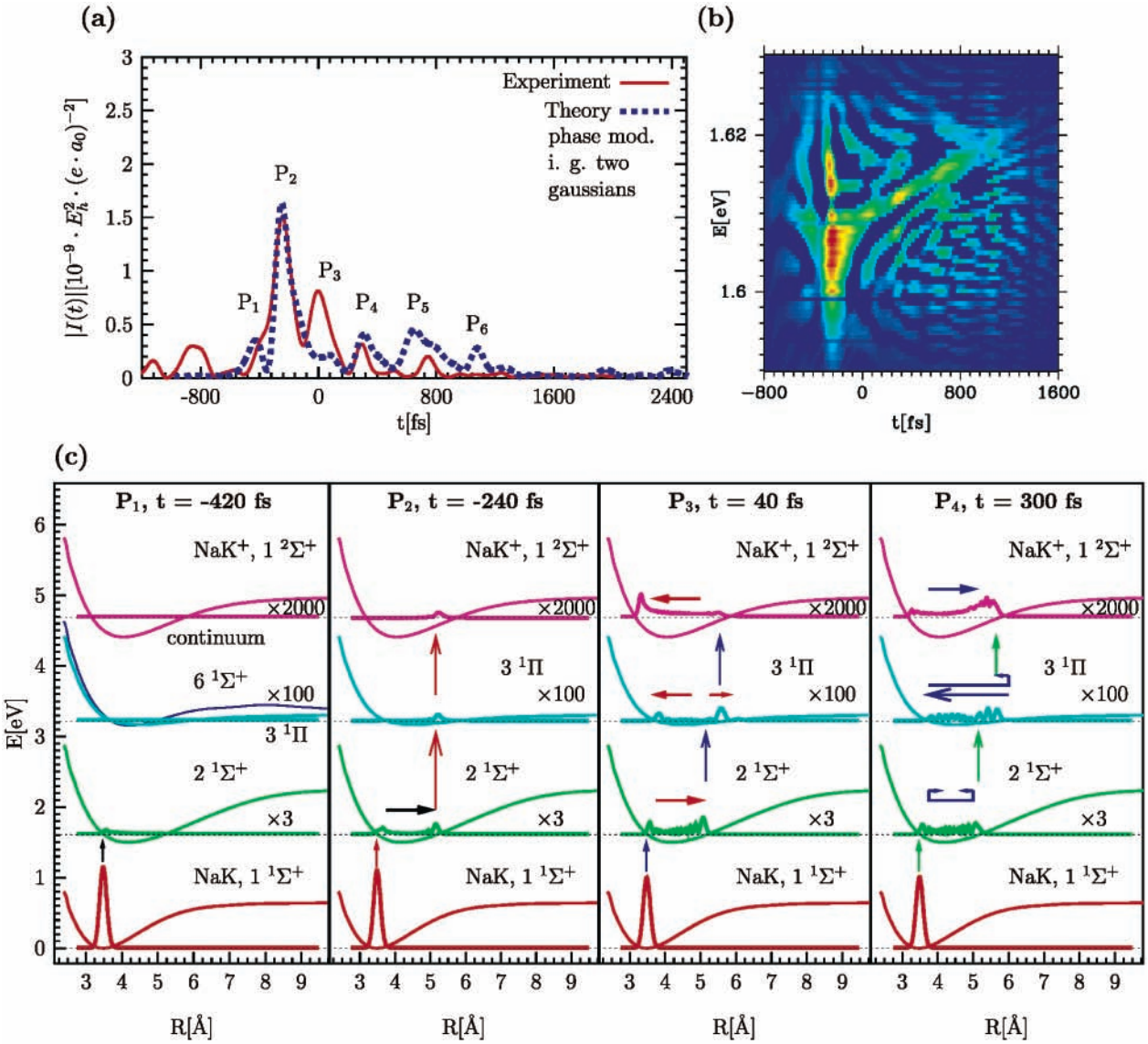

Figure 1. (a) Comparison of the theoretically (dotted line) optimized phase-modulated pulse (starting with two Gaussian pulses) with the experimentally (solid line) optimized pulse, using CLL procedure; (b) Wigner−Ville distribution of the theoretically optimized pulse; (c) snapshots of the wave-packet propagation corresponding to the times P_1 (−420 fs), P_2 (−240 fs), P_3 (40 fs), and P_4 (300 fs).

It remains an open question whether the forms of the shaped pulses can directly be used for unravelling the mechanisms of the underlying processes involved, in particular when several excited states participate. For this purpose, the robustness of the tailored laser fields has to be ensured. This can be examined by optimizing the pulses theoretically under the corresponding experimental conditions and comparing them with an optimal pulse received by inserting the experimentally obtained laser field as a starting guess in theoretical optimal control procedures. If an agreement between the pulse forms can be achieved, then the contributions of competing processes which are responsible for the pulse shapes can be revealed.

We report the joint theoretical and experimental effort to identify the processes responsible for the optimized photoionization yield in NaK from the form of the shaped pulses which have been obtained theoretically using optimal-control theory[4] and experimentally by employing the CLL algorithm.[5] On the basis of the agreement between theoretical and experimental forms of tailored fields, the conditions under which the shaped pulses are reproducible have been established and the role of different ionization pathways, e.g., direct resonant two-photon ionization vs sequential one-photon ionization has been determined.

II. Theoretical Methods and Experimental Conditions

The optimization of laser fields for controlling the photoionization in NaK has been performed in the framework of optimal-control theory formulated by Kosloff et al.[4] using full quantum-mechanical treatment. The combination of (i) electronic structure, (ii) dynamics, and (iii) optimal control considering (iv) experimental conditions will briefly be outlined.

(i) Accurate potential-energy surfaces for the ground and excited states of NaK are available in the literature[33] and have been extended by calculation of the cationic ground state necessary for the consideration of the ionization process. For this purpose, the calculations using the ab initio full CI method for the valence electrons and an effective core potential with core polarization (ECP-CPP) together with adequate atomic orbital basis sets [7s6p5d2f/5s5p4d2f] for Na and [7s5p7d2f/6s5p5d2f] for K atoms have been performed. Investigation of photoionization processes in the energy interval of 4.83 eV corresponding to three photons of 1.61 eV used in our

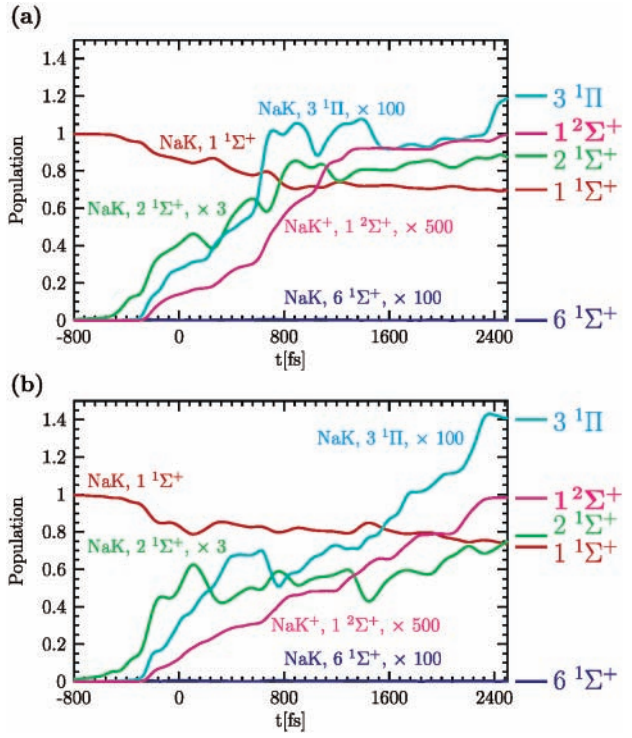

Figure 2. Time-dependent population of participating electronic states of the neutral and cationic NaK, obtained from the simulations with an initial guess using (a) two Gaussian pulses and (b) the experimentally optimized pulse.

experiments involves the three excited states $2^1\Sigma^+$, $3^1\Pi$, and $6^1\Sigma^+$ of the neutral NaK which are resonant with one- and two-photon energies, respectively.

(ii) Quantum-dynamics simulations have been carried out by representing the wave function on a grid and using a nonperturbative approach based on a Chebychev polynomial expansion of the time evolution operator. The interaction with the time-dependent electric field, which involves ground and three excited states of the neutral NaK as well as a manifold of cationic states, has been treated within the dipole approximation and using the rotating wave approximation, justified in the weak-field regime. The rotational motion has been neglected because of the large atomic masses and short time scales involved.

(iii) The objective of the optimal control is the maximization of the photoionization yield, and the target operator corresponds to the total occupation of the cationic states. For the transition dipole moments between the excited electronic states of the neutral species and the ground-state cation, different approximations have been performed.[10,11,13−16,19] We used the constant value of 5 D since it is in the range of transition dipole moments between electronic states of the neutral NaK and is sufficiently large to provide the robustness of the optimized pulses according to ref 34 and our experience. The influence of the nuclear distance-dependent transition dipole moments which are available for NaI in the literature[19] has been tested and found to be negligible.

An explicit treatment of the electronic continuum for the cationic ground state dramatically influences the optimization of the ionization process, and therefore it is mandatory for the appropriate treatment. For this purpose, the electronic continuum was discretized by introducing 14 replicas of the cationic ground state with energy differences of 95 cm^{-1} in the range from 1075 to 2310 cm^{-1} for the electron kinetic energies. This energy range covers both the direct and the sequential photoionization from the outer turning points of the involved electronic states. For the optimization of the pulses, the Krotov algorithm[35] has been employed with additional penalty factors that allow us to take into account the experimental conditions listed below.

(iv) In the experiment, NaK dimers were produced in an adiabatic coexpansion of a sodium−potassium vapor and argon carrier gas through a nozzle of 70-μm diameter into the vacuum. To obtain mainly dimers, the oven temperature and the argon pressure were set to 650 °C and to 2 bar, respectively. The femtosecond laser beam was focused onto the molecular beam in order to excite and ionize the neutral alkali dimers. The produced ions were mass selected by a quadrupole mass spectrometer and detected by a secondary electron multiplier.

The laser pulses were delivered by a Ti−sapphire oscillator (Tsunami; Spectra Physics) with a repetition rate of 80 MHz, a central wavelength of 770 nm, spectral width of 8.5 nm (full width at half maximum), and a pulse intensity of about 1 GW/cm^2 in the interaction region. Thus the experiments were carried out in the weak-field regime. These experimental conditions have been taken into account in the theoretical treatment, and the magnitude of the simulated laser field was adjusted to the experimental values according to the method given in ref 15. The pulse shaper consists of a liquid crystal modulator mask (CRI:SLM-256) with a resolution of 128 pixels located in the Fourier plane of a zero dispersion compressor. The optimized pulses were experimentally found by a nondeterministic evolutionary algorithm with phase-only modulation. For further details on the experimental setup, see ref 27. The obtained ion yields stay almost constant for repeated optimization runs, whereas the optimized pulse shapes may slightly differ. We show the best pulse form under the given experimental conditions that we have mostly obtained in the performed optimizations. The error of the optimization factor due to molecular beam fluctuation is estimated to be 5%. The temporal intensity of the acquired experimentally optimized pulse was retrieved from the experimental cross-correlation signal and served additionally as an initial guess for the theoretical optimization.

III. Optimized Pulses: Comparison between Theory and Experiment

Theoretically optimized pulses, obtained according to the procedure outlined above using two Gaussian pulses separated by 660 fs as initial guess, are shown in Figure 1a together with the experimentally optimized pulse using the CLL technique, which provides an increase of the ion yield by 60% compared to that generated by a transform limited pulse. The leading features of both phase-modulated pulses are in a good agreement. The snapshots of the wave-packet propagation under the influence of the theoretically optimized pulse (Figure 1c) serve to assign the subpulses to underlying processes and to reveal the mechanism responsible for the population of the cationic state.

The role of the P_1 subpulse is to transfer a part of the population from the ground electronic state to the first excited $2^1\Sigma^+$ state. This creates a wave packet in the $2^1\Sigma^+$ state which propagates within 180 fs almost to the outer turning point. Subsequently, at the outer turning point, the dominant P_2 subpulse simultaneously transfers the population to the $3^1\Pi$ state by a one-photon process as well as to the cationic ground state by a resonant two-photon process as can be seen from Figure 1c. In addition, the P_2 subpulse increases the population of the $2^1\Sigma^+$ state at the inner turning point. Subsequently, the P_3 subpulse brings the wave packet to the $3^1\Pi$ state after the outer turning point has been reached. In contrast to the dominant

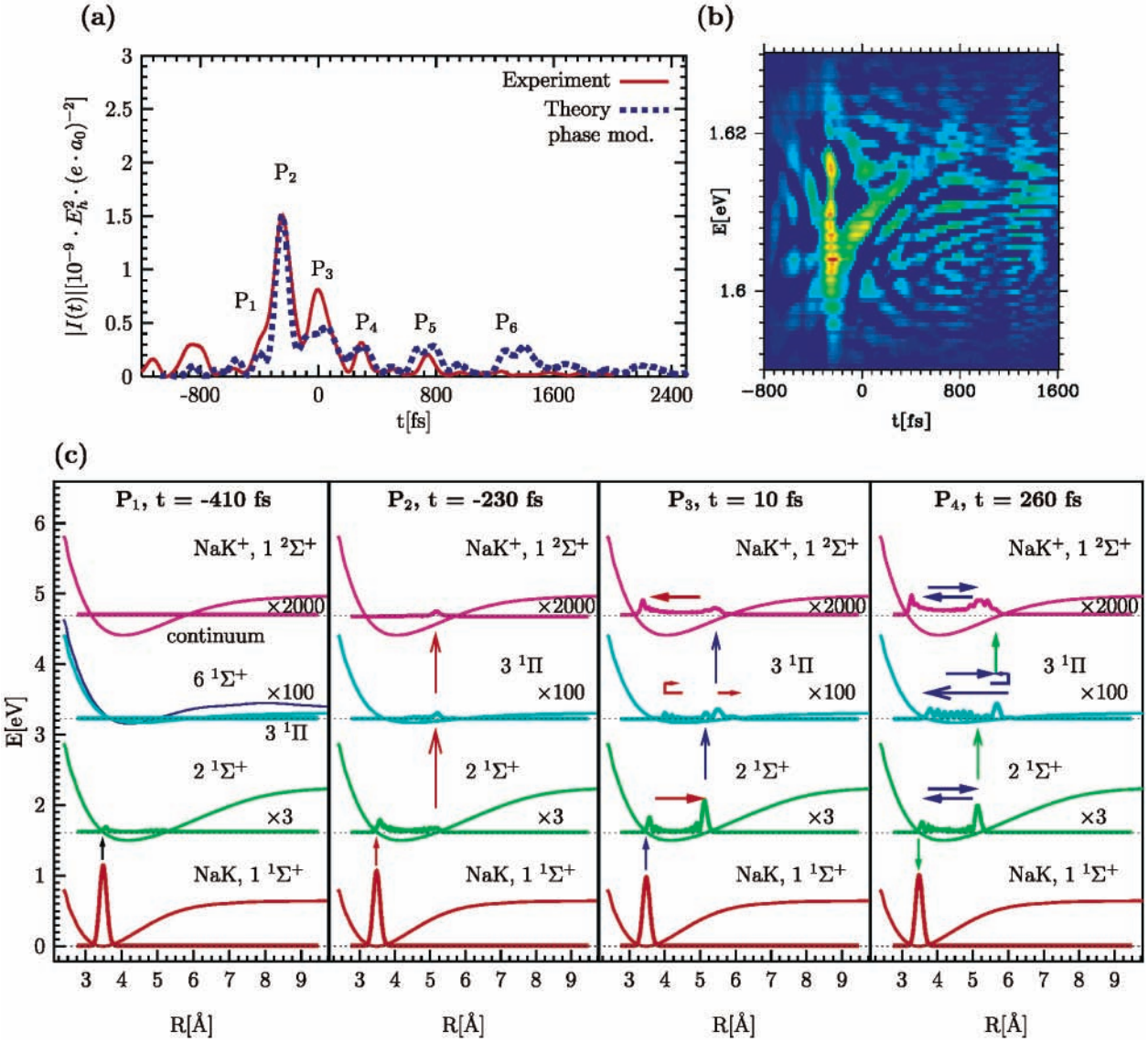

Figure 3. (a) Comparison of the theoretically (dotted line) optimized phase-modulated pulse (starting with experimentally optimized pulse) with the experimentally (solid line) optimized pulse, using CLL procedure; (b) Wigner−Ville distribution of the theoretically optimized pulse; (c) snapshots of the wave-packet propagation corresponding to P_1 (−410 fs), P_2 (−230 fs), P_3 (10 fs), and P_4 (260 fs).

subpulse P_2, the P_3 subpulse also transfers population to the cationic state by the one-photon sequential process since the split part of the wave packet, before transferred by P_2, propagates on the $3^1\Pi$ state as well. At later times, e.g., at P_4, the superposition of the wave packets complicates the propagation by interference as can be seen from the corresponding snapshot.

The separation of the early subpulses up to P_4 reflects the motion on the $2^1\Sigma^+$ state with a periodicity of ∼440 fs (oscillation period in the $2^1\Sigma^+$ state), while after the P_4 subpulse, the periodicity is disturbed by the influence of the $3^1\Pi$ state. The described steps leading to the desired population of the cationic state can be identified also from the analysis of the state populations displayed on Figure 2a. It should be noted that, besides excitation, dump processes also appear (see Figure 2a). Because of the increased population of the $2^1\Sigma^+$ and $3^1\Pi$ states, the dump processes appear at 160, 620, and 1140 fs from the $2^1\Sigma^+$ to the ground state and at 1000 and 1460 fs from the $3^1\Pi$ to the $2^1\Sigma^+$ state, and consequently, a stairlike behavior in populations of these states is present. Moreover, the P_5 subpulse causes the largest increase in the population of the cationic states, showing the important contributions of the later subpulses with low intensities.

On the basis of the above analysis of the underlying dynamics driven by the optimized pulse, we propose the following mechanism for the optimal ionization process of NaK. It involves an electronic transition followed by a direct two-photon ionization from the outer turning point of the $2^1\Sigma^+$ state. This behavior supports the proposed explanation of the experimental optimal pulse shape given in our recent publications.[30,31] However, according to the present analysis of the theoretically optimized pulses, the sequential one-photon ionization process mediated by the $3^1\Pi$ state takes over the important role at later times. The most distinct deviation from the experimental pulse form is the appearance of an early subpulse (at −870 fs), which initially populates the $2^1\Sigma^+$ state. However, this does not influence the proposed mechanism of the process.

Additional insight about the energetic and temporal structure of the optimal pulse can be gained from the Wigner−Ville representation shown in Figure 1b. The dominant feature is the increase of the photon energy with time. This upchirp in the energy regime, 1.59−1.63 eV, can be qualitatively explained by an overlap between the propagating wave packet on the $3^1\Pi$ state and the successively higher-lying vibronic levels of the cationic state. For an identification of the quantitative features,

amplitude and phase modulations would be more adequate. However, the XFROG trace obtained from our experimental result[31] also shows a pronounced upchirp in full agreement with the features displayed in Figure 1b. Moreover, the upchirp has been found to enhance the NaK ion signal according to our recent chirp-dependent experiments.[29]

To verify the robustness of theoretically optimized pulses, we have used the experimentally optimized pulse as an initial guess, and the resulting comparison is shown in Figure 3. The experimental pulse is again roughly reproduced, and the leading features of the theoretical pulse remain unchanged with respect to those obtained by taking two Gaussians as an initial guess (cf. Figure 1). The main differences between the optimized pulses obtained with distinct initial guesses concern relative intensities of the weaker subpulses, which lead only to very small relative changes of the time dependent populations (cf. Figure 2b). The Wigner−Ville representations of both theoretically optimized pulses are almost identical verifying the robustness of the derived pulses and therefore the validity of the proposed mechanism. These findings have been obtained only if the continuum of the cationic state has been taken into account as described above.

IV. Summary

The agreement between experimentally and theoretically optimized pulses, which is independent from the initial guess, achieved in this contribution, shows that the shapes of the pulses can be used to deduce the mechanism of the processes underlying the optimal control. In the case of the optimization of the ionization process in NaK, this involves a direct two-photon resonant process followed by a sequential one-photon process at a later time.

These findings obtained on the simple system are promising for using the shapes of tailored pulses to reveal the nature of processes involved in the optimal control of more complex systems.

Acknowledgment. We thank Prof. R. Kosloff for giving us access to his optimal-control algorithms. This work has been supported by the Deutsche Forschungsgemeinschaft in the framework of the Sonderforschungsbereich 450: Analyse und Steuerung photoinduzierter ultraschneller Reaktionen.

References and Notes

(1) Brumer, P.; Shapiro, M. *Chem. Phys. Lett.* **1986**, *126*, 541.
(2) Rice, S. A. *Science* **1992**, *258*, 412.
(3) Peirce, A. P.; Dahleh, M. A.; Rabitz, H. *Phys. Rev. A* **1988**, *37*, 4950.
(4) Kosloff, R.; Rice, S. A.; Gaspard, P.; Tersigni, S.; Tannor, D. J. *Chem. Phys.* **1989**, *139*, 201.
(5) Judson, R. S.; Rabitz, H. *Phys. Rev. Lett.* **1992**, *62*, 1500.
(6) Assion, A.; Baumert, T.; Bergt, M.; Brixner, T.; Kiefer, B.; Seyfried, V.; Strehle, M.; Gerber, G. *Science* **1998**, *282*, 919.
(7) Brixner, T.; Gerber, G. *ChemPhysChem.* **2003**, *4*, 418.
(8) Lewis, R.; Menkir, G. M.; Rabitz, H. *Science* **2001**, *292*, 709.
(9) Daniel, C.; Full, J.; Gonzáles, L.; Lupulescu, C.; Manz, J.; Merli, A.; Vajda, Š.; Wöste, L. *Science* **2003**, *299*, 536.
(10) Braun, M.; Engel, V. *Z. Phys. D* **1997**, *39*, 301.
(11) Schwoerer, H.; Pausch, R.; Heid, M.; Engel, V.; Kiefer, W. *J. Chem. Phys.* **1997**, *107*, 9749.
(12) Shen, Z. W.; Chen, T.; Heid, M.; Kiefer, W.; Engel, V. *Eur. Phys. J. D* **2001**, *14*, 167.
(13) de Vivie-Riedle, R.; Kobe, K.; Manz, J.; Meyer, W.; Reischl, B.; Rutz, S.; Schreiber, E.; Wöste, L. *J. Phys. Chem.* **1996**, *100*, 7789.
(14) Nicole, C.; Bouchène, M. A.; Meier, C.; Magnier, S.; Schreiber, E.; Girard, B. *J. Chem. Phys.* **1999**, *111*, 7857.
(15) Pesce, L.; Amitay, Z.; Uberna, R.; Leone, S. R.; Ratner, M.; Kosloff, R. *J. Chem. Phys.* **2001**, *114*, 1259.
(16) Sundermann, K.; de Vivie-Riedle, R. *J. Chem. Phys.* **1999**, *110*, 1896.
(17) Hornung, T.; Motzkus, M.; de Vivie-Riedle, R. *J. Chem. Phys.* **2001**, *115*, 3105.
(18) Hornung, T.; Motzkus, M.; de Vivie-Riedle, R. *Phys. Rev. A* **2002**, *65*, 021403.
(19) Grégoire, G.; Mons, M.; Dimicoli, I.; Piuzzi, F.; Charron, E.; Dedonder-Lardeux, C.; Jouvet, C.; Martrenchard, S.; Solgadi, D.; Suzor-Weiner, A. *Eur. Phys. J. D* **1998**, *1*, 187.
(20) Shen, Z.; Engel, V.; Xu, R.; Cheng, J.; Yan, Y. *J. Chem. Phys.* **2002**, *117*, 6142.
(21) Rodriguez, G.; Eden, J. G. *Chem. Phys. Lett.* **1993**, *205*, 371.
(22) Rodriguez, G.; John, P. C.; Eden, J. G. *J. Chem. Phys.* **1995**, *103*, 10473.
(23) Pausch, R.; Heid, M.; Chen, T.; Kiefer, W.; Schwoerer, H. *J. Chem. Phys.* **1999**, *110*, 9560.
(24) Pausch, R.; Heid, M.; Chen, T.; Schwoerer, H.; Kiefer, W. *J. Raman Spectrosc.* **2000**, *31*, 7.
(25) Uberna, R.; Amitay, Z.; Loomis, R. A.; Leone, S. R. *Faraday Discuss.* **1999**, *113*, 385.
(26) Bartelt, A.; Minemoto, S.; Lupulescu, C.; Vajda, Š.; Wöste, L. *Eur. Phys. J. D* **2001**, *16*, 127.
(27) Vajda, Š.; Bartelt, A.; Kaposta, C.; Leisner, T.; Lupulescu, C.; Minemoto, S.; Rosendo-Francisco, P.; Wöste, L. *Chem. Phys.* **2001**, *267*, 231.
(28) Vajda, Š.; Lupulescu, C.; Bartelt, A.; Budzyn, F.; Rosendo-Francisco, P.; Wöste, L. In *Femtochemistry and Femtobiology*; Douhal, A., Santamaria, J., Eds.; World Scientific Publishing: Singapore, 2002; p 472.
(29) Bartelt, A.; Lindinger, A.; Lupulescu, C.; Vajda, Š.; Wöste, L. *Phys. Chem. Chem. Phys.* **2003**, *5*, 3610.
(30) Lupulescu, C.; Lindinger, A.; Plewicki, M.; Merli, A.; Weber, S. M.; Wöste, L. *Chem. Phys.* **2004**, *296*, 63.
(31) Bartelt, A. Steuerung der Wellenpaketdynamik in kleinen Alkaliclustern mit optimierten Femtosekundenpulsen, Ph.D. Thesis, Freie Universität Berlin, 2002.
(32) Ballard, J. B.; Stauffer, H. U.; Amitay, Z.; Leone, S. R. *J. Chem. Phys.* **2002**, *116*, 1350.
(33) Magnier, S.; Aubert-Frécon, M.; Millié, P. J. *Mol. Spectrosc.* **2000**, *200*, 96
(34) Demiralp, M.; Rabitz, H. *Phys. Rev. A* **1998**, *57*, 2420.
(35) Krotov, V. F. *Control Cybernetics* **1988**, *17*, 115.